The Variation of MAP-MRI –derived Parameters along White Matter Fiber Pathways in the Human Brain

Alexandru V Avram[1], Alan S Barnett[1,2], and Peter J Basser[1]

[1]*Section on Tissue Biophysics and Biomimetics, NICHD, National Institutes of Health, Bethesda, MD, United States,* [2]*The Henry Jackson Foundation, Bethesda, MD, United States*

Target audience: MR scientists and clinicians; radiologists; neuroscientists;

Introduction: Pathway-specific changes of diffusion tensor imaging (DTI)-derived parameters (e.g., Fractional Anisotropy (1), radial diffusivity) are associated with normal variations in cognitive performance and changes during neurological disorders, neurodegenerative pathologies, and aging. Nevertheless, the microstructural characterization provided by DTI is incomplete. Recently, a novel framework was proposed as a generalization of DTI, to provide a more comprehensive white matter assessment by measuring the mean apparent diffusion propagator (MAP). In MAP-MRI (2) the propagator can be conveniently characterized using scalar descriptors, such as zero-displacement probabilities, non-gaussianity, and propagator anisotropy (2), which can also be decomposed along the axes of the local anatomical reference frame (given by the diffusion tensor). Since the local anatomical orientation varies along the fiber, care should be used when interpreting these indices. In this study we quantify the diffusion properties of cerebral white matter (WM) in healthy volunteers using MAP-MRI, describe the variation of scalar descriptors of the propagator along the major white matter pathways, and discuss their the clinical and biological significance.

Methods: We scanned three healthy volunteers on a 3T MRI scanner using spin-echo diffusion-weighted EPI with full brain coverage, 3mm slice thickness, image matrix size 70x70, field-of-view 21x21cm^2, SENSE factor 2, and TE/TR=94/5800ms. For each subject, 600 DWIs were acquired with multiple orientations sampling the sphere for each of the 6 b-values (b_{max}=6,000 s/mm^2). The diffusion gradient pulse width and separation were δ=34ms and Δ=41ms, respectively and G_{max}=4.93G/cm. In the same session, a 1mm isotropic MP-RAGE scan was also obtained to serve as an anatomical template for image registration and region-of-interest (ROI) segmentation. After motion and eddy current correction (3) of all DWIs, MAP-MRI was used to measure the propagator and derive scalar descriptors, e.g, return-to-origin probability (RTOP), return-to-axis probability (RTAP), return-to-plane probability (RTPP), total, perpendicular and parallel non-gaussianity indices (NG, $NG_{\perp}$, and $NG_{||}$ respectively) and propagator anisotropy measures (2). To visualize white matter fiber pathways, probabilistic fiber tractography was performed (4), and different fiber bundles were defined based on anatomical ROIs. In each bundle, the fiber tracks were resampled to have the same number of points, and mean MAP parameters were plotted along the fibers.

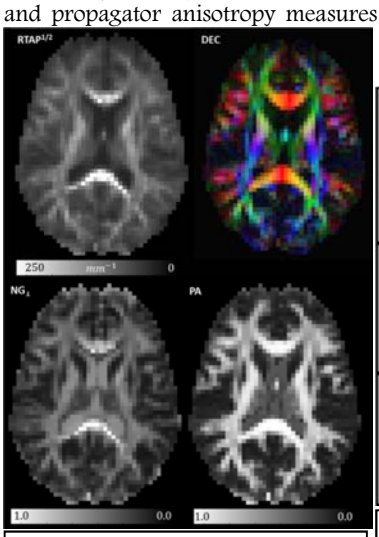

Figure 1: Images of MAP-MRI derived parameters: RTAP, $NG_{\perp}$, and PA.

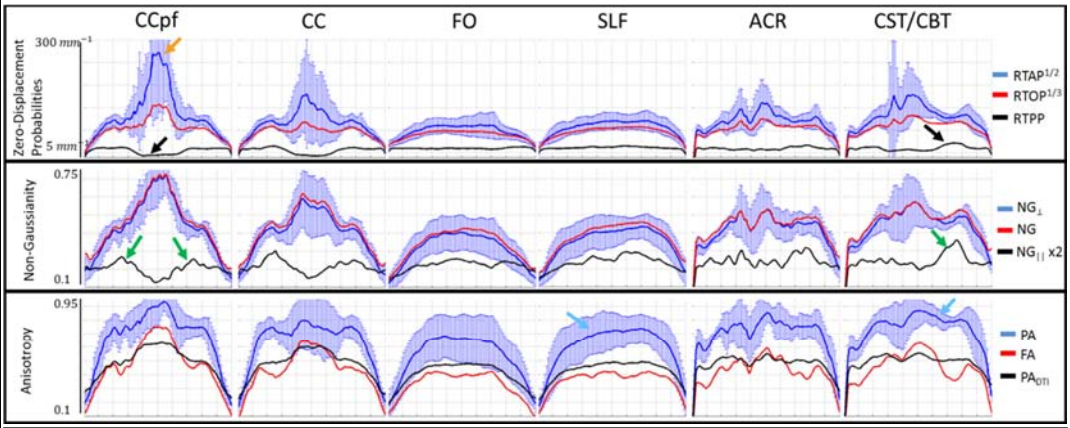

Figure 2: Average variation of MAP-MRI parameters along major white matter fiber pathways: posterior forceps of the corpus callosum (CCpf), CC, Fronto-occipital Fasciculus (FO), Superior Longitudinal Fasciculus (SLF), Anterior Corona Radiata (ACR), Corticospinal/Corticobulbar Tracts (CST/CBT). Error bars are shown for RTAP$^{1/2}$, $NG_{\perp}$, and PA.

Results and Discussion: MAP-MRI-derived scalar indices were consistent across all subjects, revealing similar whole-brain spatial variations, which were within the expected ranges (Fig.1). Under certain conditions (2), zero-displacement probabilities are inversely related to the spatial dimensions of restrictions: mean pore cross-sectional area (RTAP) and volume (RTOP). Fig.2 shows quite large variations of these indices along the projection (ACR,CST/CBT) and commissural pathways (CCpf, CC), mainly due to different levels of fiber coherence along these fibers, with the largest values occurring in the medial splenium (Fig.2, orange arrow) of the CC (also Fig.1). The RTPP has a narrower dynamic range with larger values in regions of crossing fibers and smaller values in regions of highly coherent fibers (Fig.2, black arrows). NG quantifies deviations of the propagator from Gaussian diffusion and is dominated by contributions from diffusion perpendicular to the local tissue orientation $NG_{\perp}$ (Fig.2). Axial diffusion is more non-Gaussian (larger $NG_{||}$) in regions of crossing fibers (Fig.2, green arrows). The propagator anisotropy (PA) quantifies the dissimilarity of the propagator relative to its isotropic counterpart and shows larger values compared to the FA with smaller variations due to crossing fibers (Fig.2, blue arrows), while the PA_{DTI} is derived from the low order MAP coefficients and is similar to the FA in DTI (Fig.2). Along associative pathways (FO/SLF) the MAP parameters lacked large variations suggesting that these regions are rather amenable to be characterized with WM ROI analysis. Finally, it is important to note that even though the anatomical reference frame along which the MAP is expanded with orthogonal basis functions does not affect the estimation of the MAP or RTOP, measures of non-Gaussianity and anisotropy are expected to be more sensitive to the choice of the reference frame (which is used to characterize Gaussian diffusion).

Conclusion: MAP MRI parameters must be interpreted with care, especially when analyzing their projections along the axes of the local anatomical reference frame (similarly to analyzing axial and radial diffusivities in DTI). Relative variations of MAP-MRI parameters along specific pathways (i.e., contralateral projection pathway internal control) could provide powerful new clinical biomarkers in assessing the microstructural integrity and connectivity for disease progression and treatment response monitoring.

References: 1. Basser & Pierpaoli, JMR 1996;111:209-219; 2. Özarslan et al., Neuroimage 2013;78:16-32; 3. Pierpaoli et al., ISMRM 2010;#1597; 4. Tournier et al., Neuroimage 2007;35:1459-72;